



Published in final edited form as:

Mucosal Immunol. 2020 May ; 13(3): 471–480. doi:10.1038/s41385-019-0238-1.

Antibiotic-induced microbiome perturbations are associated with significant alterations to colonic mucosal immunity in rhesus macaques

Jennifer A. Manuzak^{1,2,3,*}, Alexander S. Zevin^{1,2,*}, Ryan Cheu^{1,2,3}, Brian Richardson⁴, Jacob Modesitt^{1,2}, Tiffany Hensley-McBain^{1,2}, Charlene Miller^{1,2,3}, Andrew T. Gustin^{1,2,5}, Ernesto Coronado^{1,2}, Toni Gott^{1,2}, Mike Fang⁴, Michael Cartwright⁴, Solomon Wangari², Brian Agricola², Drew May², Elise Smith⁵, Hans Benjamin Hampel^{6,7}, Michael Gale^{2,5}, Cheryl M. Cameron⁸, Mark J. Cameron⁴, Jeremy Smedley^{2,9}, Nichole R. Klatt^{1,2,3}

¹Department of Pharmaceutics, University of Washington, Seattle, WA, USA ²Washington National Primate Research Center, Seattle, WA, USA ³Department of Pediatrics, Miller School of Medicine, University of Miami, Miami, FL, USA ⁴Department of Population and Quantitative Health Sciences, Case Western Reserve University, Cleveland, OH, USA ⁵Department of Immunology, University of Washington, Seattle, WA, USA ⁶Division of Infectious Diseases and Hospital Epidemiology, University Hospital Zurich ⁷Department of Public Health, Epidemiology, Biostatistics and Public Health Institute, University of Zurich, Zurich, Switzerland ⁸Department of Pathology, Case Western Reserve University, Cleveland, OH, USA ⁹Oregon National Primate Research Center, Beaverton, OR, USA

Abstract

The diverse bacterial communities that colonize the gastrointestinal tract play an essential role in maintaining immune homeostasis through the production of critical metabolites such as short chain fatty acids (SCFA), and this can be disrupted by antibiotic use. However, few studies have addressed the effects of specific antibiotics longitudinally on the microbiome and immunity. We evaluated the effects of four specific antibiotics; enrofloxacin, cephalexin, paromomycin, and clindamycin; in healthy female rhesus macaques. All antibiotics disrupted the microbiome, including reduced abundances of fermentative bacteria and increased abundances of potentially pathogenic bacteria, including *Enterobacteriaceae* in stool, and decreased *Helicobacteraceae* in the colon. This was associated with decreased SCFAs, indicating altered bacterial metabolism. Importantly, antibiotic use also substantially altered local immune responses, including increased neutrophils and Th17 cells in the colon. Furthermore, we observed increased soluble-CD14 in plasma, indicating microbial translocation. These data provide a longitudinal evaluation of

Users may view, print, copy, and download text and data-mine the content in such documents, for the purposes of academic research, subject always to the full Conditions of use:http://www.nature.com/authors/editorial_policies/license.html#terms

Author Contributions

Study design: NRK, JS, ASZ; Animal studies: JS, DM, SW, BA; Sample processing: ASZ, JAM, CM, EC, TG, ATG; Experimental analysis: ASZ, JAM, RC, THM, CM, ATG, BR, MF, MC, ES; Data analysis: JAM, ASZ, THM, MC, CMC, MJC, MG; Consulting on clinical antibiotics use: HBH; Manuscript preparation and editing: JAM, ASZ, HBH, MJC, NRK.

*J.A.M and A.S.Z. contributed equally to this work.

antibiotic-induced changes to the composition and function of colonic bacterial communities, associated with specific alterations in mucosal and systemic immunity.

Introduction

The mammalian gastrointestinal (GI) tract is densely colonized with diverse bacterial communities, which are critical in human health, and contribute to maintenance of mucosal and systemic immune homeostasis¹. Furthermore, compounds derived from the GI microbiota play key roles in promoting proper host immune function. Short chain fatty acids (SCFA), produced exclusively through microbial fermentation of dietary fibers in the colon, act through a variety of mechanisms to promote mucosal health. For example, butyrate is a key energy source for colonic epithelial cells and also influences gene expression by acting as a histone deacetylase inhibitor².

In many disease states, there is an observed alteration to the abundance and diversity of the bacterial species in these communities when compared to healthy controls. One example is that of human immunodeficiency virus (HIV) infection, which has been associated with increased abundances of Proteobacteria and reduced abundances of *Bacteroides*. Aside from changes in bacterial community composition, HIV infection is associated with altered host-microbiota interactions. Specifically, impaired mucosal immunity and breaches in the epithelium lead to translocation of microbes and microbial products (microbial translocation – MT) from the colonic lumen into systemic circulation, which is associated with aberrant immune activation, and increased morbidity and mortality³⁻⁷.

Nonhuman primates (NHP) are an extremely important model for critical research pertaining to human health, such as aging, viral hepatitis infection, Zika virus infection, and HIV infection⁸⁻¹⁰. Indeed, simian immunodeficiency virus (SIV) infection of macaques has been essential for understanding the pathogenesis of HIV infection. As in humans, NHP demonstrate colonic microbiota dysbiosis and MT during SIV infection¹¹⁻¹⁵, which has provided a detailed understanding of the consequences of MT, such as liver damage resulting from increased immune activation in response to increased burden of microbial products¹⁶. SIV infection of NHP has also been critical for evaluating vaccines and therapeutic approaches¹⁷. As more NHP studies are beginning to incorporate microbiome analyses, it is important to develop a detailed understanding of the composition of NHP microbiota and the effects of xenobiotics on these communities.

Antibiotics are important xenobiotics that are widely used in NHP veterinary and human health care, but are known to disrupt native microbiota¹⁸. Due to the extensive interaction of the microbiota with the host immune system, these antibiotic-mediated alterations to the microbiota composition can result in distinct immunological consequences. For example, antibiotic treatment in mice resulted in increased inflammation as a result of increased MT and increased mucosal immune activation in the colon^{19, 20}. Other murine models have demonstrated that administration of antibiotics early in life can increase incidence of autoimmune disorders²¹. Indeed, our group previously demonstrated that antibiotics altered mucosal bacterial communities in SIV-infected rhesus macaques (RM)^{17, 22}. However, due to the SIV-infection we were unable to attribute any immunological changes to the

antibiotics alone. Thus, the impact of antibiotic treatments on the microbiota and mucosal immunity in NHP models has not been thoroughly evaluated, despite the importance of this model for human disease.

Here, we assess the impact of four commonly used antibiotics on colonic microbiota and mucosal immunity in healthy RM: (i.) Cephalexin, a beta-lactam antibiotic commonly used to treat a variety of gram-positive bacterial infections including skin and soft tissue infections²³ and part of a class of antibiotics, first generation cephalosporins, widely used as prophylactic antibiotics in surgical procedures in macaques; (ii.) Clindamycin, a lincosamide antibiotic used for a plethora of human conditions including acne, soft tissue infections, second-line strep throat treatment, bacterial vaginosis, and methicillin resistant *Staphylococcus aureus* (MRSA) infection^{24, 25}, and recognized by primate veterinarians for its potential to induce mild colitis; (iii.) Paromomycin, an aminoglycoside antibiotic commonly used in HIV-infected individuals for Cryptosporidium infections²⁶ and for its extremely low absorption confining its effects to the GI tract; (iv.) Enrofloxacin is a fluoroquinolone antibiotic commonly used in veterinary practice and given often to NHPs prophylactically for medical studies²⁷. We demonstrate that all four antibiotics disrupted the native microbiota, leading to reduced concentrations of fecal SCFA, and that this was linked to an infiltration of neutrophils and IL-17 producing cells in the colonic mucosa. These data are the first to demonstrate the longitudinal effects of multiple antibiotic treatments on microbial composition, mucosal immunity, bacteria fermentation, inflammation, and microbial translocation.

Materials and Methods

Study animals and antibiotic treatment

Animals were housed and cared for in Association for the Assessment and Accreditation of Laboratory Animal Care international (AAALACi) accredited facilities, and all animal procedures were performed according to protocols approved by the Institutional Animal Care and Use Committee (IACUC) of University of Washington (Protocol 4304–16). None of the animals included in this study received antibiotics within 6 months prior to the start of the study. Twelve female rhesus macaques were treated with antibiotics (n=3/group) including: enrofloxacin (12 mg/kg, n=3, once daily, 9 days), cephalexin (30 mg/kg, n=3, once daily, 9 days), paromomycin (25 mg/kg, n=3, twice daily, 9 days), or clindamycin (10 mg/kg, n=3, twice daily, 6 days). We collected blood, biopsies of the mid descending colon approximately 20–30 cm from the anus, and stool before, during, and after the antibiotic treatment according to the study schedule in (Figure 1). Stool and two biopsies were stored at –80°C immediately upon collection. We also stored one biopsy from each animal at each time point in RNALater solution. Blood and the remaining biopsies were processed immediately after collection as described below. None of the animals had any clinical complications related to the antibiotic treatment.

DNA extraction, 16S rRNA gene sequencing and data analysis

We extracted DNA from cryopreserved stool and colon biopsies using the PowerFecal DNA Isolation Kit (Qiagen, Valencia, CA). We then prepared sequencing libraries as described by

the Earth Microbiome Project²⁸ and sequenced them using the Illumina MiSeq Sequencer (Illumina, San Diego, CA). All sequence reads and operational taxonomic unit (OTU) observations were included in our analyses, in order to maximize the observed diversity of the bacterial communities. Sequencing data was analyzed using the QIIME software²⁹. We clustered OTUs at 97% similarity using the SWARM algorithm³⁰ and assigned taxonomy based on sequence similarity to the SILVA database³¹. We calculated alpha diversity using the Inverse Simpson Index, beta diversity using Bray-Curtis dissimilarity, and performed principal coordinates analysis (PCoA) using the *ape* and *vegan* packages in R. Sequences have been submitted to the NCBI SRA (accession number PRJNA604177).

Gas Chromatography-Mass Spectrometry

We first weighed 0.05–0.1 g of stool into a sterile microcentrifuge tube and suspended the stool in acidified water (pH 2.5) at a concentration of 0.1 g/mL, vortexed thoroughly, and centrifuged at maximum speed for 10 minutes. We then transferred 250µL of the supernatant to a fresh microcentrifuge tube and added 50µL of an 800µM solution of 2-methyl valeric acid in acidified water, which served as an internal standard. We next added 300µL of ethyl acetate, vortexed for two minutes, and then centrifuged at maximum speed for 10 minutes. We then transferred 100µL of the organic phase into an autosampler vial and analyzed SCFA concentrations on a Shimadzu QP2010 GCMS (Shimadzu, Kyoto, Japan). We used a Stabilwax fused silica column (30m × 0.32mm × 0.25 mm, Restek Bellefonte, PA) with helium as the mobile phase with a linear velocity of 47.2 cm/sec. The method started at 90°C and increased at a rate of 10°C/min to 180°C and then at a rate of 20°C/min to 250°C, and held at that temperature for 2 minutes. We used solutions of acetic, propionic, butyric, isobutyric, valeric, and isovaleric acids (Sigma Aldrich, St. Louis, MO) in ethyl acetate as calibration standards.

Blood and tissue processing

We collected blood in Vacutainer tubes (BD, Franklin Lakes, NJ) and transported immediately to the lab. We then centrifuged the whole blood at 2,000 RPM for 10 minutes at 24°C to separate cells and plasma, then collected 1 mL aliquots of plasma and stored them at –80°C. We stored biopsies in RPMI 1640 medium (GE Healthcare Life Sciences, Pittsburgh, PA) upon collection and immediately transported them to the laboratory. We stored two biopsies at –80°C and one in RNALater solution as noted above for DNA extraction and RNAseq analysis, respectively. We placed the remaining biopsies into 50mL RPMI medium supplemented with 1X Pennicillin/Streptomycin (GE Healthcare Life Sciences), 40 µg/mL Liberase TL (Sigma Aldrich), and 4 µg/mL DNase (Sigma Aldrich) and vigorously stirred at 37°C for one hour. We then manually dissociated the digested biopsy tissue into a single cell suspension by grinding them across a sterile 40µm mesh filter. We then centrifuged the cells at 1,900 RPM for 6 minutes at 4°C, suspended them in 8mL RPMI 1640 supplemented with 10% FBS, and 1X Pennicillin/Streptomycin (R10), and divided this suspension evenly between two 5mL round-bottom tubes for flow cytometry analysis.

Antibody staining and flow cytometry

Innate and adaptive immunophenotyping: We stained one tube of the single cell suspensions immediately after processing in each tissue and blood. We first washed the cells in 4mL of sterile PBS and stained them with the LIVE/DEAD Fixable Aqua Dead Cell Stain Kit (ThermoFisher Scientific, Waltham, MA) for 5 minutes at room temperature. We then stained the cells with the following surface antigen antibodies, all of which were obtained from BD Biosciences (San Jose, CA) unless otherwise stated, for 20 minutes at 4°C: CD45-PerCP (clone D058–1283), CD-11b-APC-H7 (clone ICRF44), CCR6-Pe (clone 11A9), CD3-Pe-CF594 (clone SP34–2), CD20-Pe-Cy5 (clone 2H7), PD-1 (eBioscience, San Diego, CA, clone eBioJ105), CD274 (Biolegend, San Diego, CA, clone 29E.2A3), CD8-BV570 (Biolegend clone RPA-T8), CD4-BV605 (Biolegend clone OKT4), CD16-BV650 (clone 3G8), HLA-DR-BV711 (clone G46–6), and CD14-BV785 (clone M5E2). We next washed the cells in sterile PBS and permeabilized them using BD Cytfix/Cytoperm for 20 minutes at 4°C. We then washed the cells two times in BD Perm/Wash buffer and stained them with the following intracellular antigen antibodies all of which were obtained from BD Biosciences unless otherwise stated, for 20 minutes at 4°C: Ki67-FITC (clone B56), IL-23-eFLuor660 (eBioscience clone 23dcdp), Arginase-1-Ax700 (R&D Systems, Minneapolis, MN, clone 658922), and Caspase-3-V450 (clone C92–605). We then fixed the cells in 1% paraformaldehyde solution (Sigma Aldrich). Data is shown only for significantly altered parameters.

Intracellular cytokine staining: We stimulated the second tube of the single cell suspension with 10 ng/mL phorbol myristate acetate (Sigma Aldrich) and 1 µg/mL ionomycin (Life Technologies) in 2 mL R10 supplemented with 1 mg/mL brefeldin A for 16 hours at 37°C. We then washed the cells with 4 mL sterile PBS and stained them with the LIVE/DEAD Fixable Aqua Dead Cell Stain Kit (ThermoFisher Scientific, Waltham, MA) for 5 minutes at room temperature. We then stained the cells with the following surface antigen antibodies, all of which were obtained from BD Biosciences (San Jose, CA) unless otherwise stated, for 20 minutes at 4°C: CD45-PerCP (clone D058–1283), CD8-APC-H7 (clone SK1), CD3-PE-CF594 (clone SP34–2), CD11b-PE-Cy5 (clone ICRF44), CD11c-PE-Cy7 (eBioscience clone 3.9), CD20-BV570 (Biolegend clone 2H7), CD4-BV605 (Biolegend clone OKT4), HLA-DR-BV711 (clone G46–6), and CD14-BV785 (clone M5E2). We then washed the cells in sterile PBS and permeabilized them using BD Cytfix/Cytoperm for 20 minutes at 4°C. We then washed the cells twice in BD Perm/Wash buffer and stained them with the following intracellular antigen antibodies all of which were obtained from BD Biosciences unless otherwise stated, for 20 minutes at 4°C: IL6-FITC (MQ2–6A3), GM-CSF-APC (Biolegend clone BVD2–21C11), TNF-α-AF700 (clone Mab11), IL-17-Pe (eBioscience clone eBio64CAP17), IL-22-PerCP-efluor 710 (eBioscience clone IL022JOP), IL-8-BV421 (clone G265–8), and IFNγ-BV650 (Biolegend clone 4S.B3). We then fixed the cells in 1% paraformaldehyde solution (Sigma Aldrich). We collected stained cells on an LSR II flow cytometer (BD Biosciences) and analyzed the data using FlowJo software (v10.2, FlowJo LLC, Ashland, OR).

RNA sequencing

We isolated total RNA from colonic biopsies stored in RNALater solution using Qiagen RNeasy Micro Kits (Qiagen, Valencia, CA). We then generated sequencing libraries using TruSeq Stranded Total RNA with Ribo-Zero Globin kits (Illumina, San Diego, CA) and 200ng of RNA as the input. We then sequenced the libraries on an Illumina HiSeq 2500 Sequencer (Illumina). We trimmed the raw sequence reads of adapters and filtered them using skewer to discard reads with an average phred quality score of less than 30 or a length of less than 36. Trimmed reads were then aligned using the HISAT2³² aligner to the NCBI reference Mmul macaque genome (Mmul_8.0.1) and sorted using SAMtools³³. Aligned reads were counted and assigned to gene meta-features using featureCounts³⁴ as part of the Subread package. Sequence and gene expression data are available at the Gene Expression Omnibus (accession number GSE143729).

ELISA

We used the Human soluble CD14 Quantikine ELISA Kit (R&D Systems, Minneapolis, MN) to quantify plasma concentrations of sCD14 before, during, and after the antibiotic treatment according to the manufacturer's instructions. We diluted plasma 1:200 prior to analysis.

Statistical Analyses

Given the similarities in response to the different antibiotics classes, the twelve animals were grouped for statistical analysis longitudinally prior to and after antibiotic treatment. We conducted paired t-tests across all twelve animals to determine statistical differences between SCFA concentrations and immunological data, including flow cytometry and ELISA. To evaluate statistical differences in bacterial abundances, we utilized the Wilcoxon signed-rank test using the abundance for each bacterial species at each time point. All statistics were corrected for multiple comparisons using a post-hoc Bonferroni Correction. We performed these analyses using GraphPad Prism (v5.0 GraphPad, La Jolla, CA). For our RNA-Seq analysis approach, we imported the count files into R and performed quality control, normalization and analysis using the generalized linear model likelihood ratio test for pairwise differential gene expression testing between timepoints and treatments implemented in Bioconductor's edgeR³⁵. Gene Set Variation Analysis (GSVA)³⁶ was used for pathway enrichment analysis with subsequent testing of significantly differentiated pathways using LIMMA's³⁷ moderated t-statistic. P-values for both the gene expression analysis and pathway enrichment were calculated with a maximum nominal P 0.05 chosen as significant. Longitudinal gene expression and pathway enrichment figures were generated using the ggplot2 library³⁸.

Results

Antibiotics disrupt microbiota in the colonic mucosa and stool

We used 16S rRNA gene sequencing to profile the bacterial communities in the colonic mucosa and stool before, during, and after the antibiotic treatments. Prior to the antibiotic treatment (Days -42 and -21), the colon mucosa of all animals was dominated by

Helicobacteraceae (average 67.1%, range 5.6%–99%), with minor populations of *Ruminococcaceae* (average 7%), *Prevotellaceae* (average 6.9%), *Lachnospiraceae* (average 2.7%), and *Spirocheateceae* (average 2.7%), in strong agreement with our and other groups' data on the microbiota associated with the colon mucosa in rhesus macaques^{22, 39} (Figure 2A). Rapidly after antibiotic treatment (Day 3), there was a significant decrease in the abundance of the dominant *Helicobacteriaceae* ($P=0.0161$) with increased abundances of *Prevotellaceae* and *Ruminococcaceae*, although there was no change in the abundance of these bacteria due to treatment with clindamycin. After the antibiotic treatments had ended (Days 14, 28, and 63), the mucosal bacterial communities generally returned to the pre-antibiotics state, with high abundances of *Helicobacteriaceae*, but the rate and extent of this recovery differed between the three groups that showed a response to the antibiotic treatment. Specifically, administration of paromomycin appeared to have longer-lasting effects than did the other antibiotics.

We next evaluated the stool-associated bacterial communities (Figure 2B). Prior to the antibiotic treatment, all of the animals showed high abundances of *Prevotellaceae* and *Ruminococcaceae* among other, smaller populations of Firmicutes and Bacteroidetes bacteria. All four antibiotics disrupted composition of the stool microbiota, but these effects were less pronounced and more variable than those observed in the mucosa. Thus, we used the random forests classifier to determine which bacterial groups were most discriminative between time points with and without antibiotics. We found that the abundances of *Enterobacteriaceae* and *Verrucomicrobiaceae* were the most discriminative between the three time points, followed by *Succinivibrionaceae*, *Streptococcaceae*, and *Helicobacteriaceae* (Figure 2C). We evaluated the genera detected from the family *Enterobacteriaceae*, and found that it was predominantly *Escherichia*, with lower abundances of *Proteus*, *Enterobacter*, and *Klebsiella* (Figure 2D). The abundance of bacteria from the family *Enterobacteriaceae* was low before the antibiotic treatment, but rapidly increased during the antibiotic treatment, and remained increased following cessation of antibiotic treatments (Figure 2E). We also found that the abundance of *Verrucomicrobiaceae*, which was determined to be an *Akkermansia* sp. was significantly increased during the antibiotic treatment and remained increased after the treatments ended (Figure 2F). We also observed decreased abundances of *Ruminococcaceae*, one of the key types of fermentative bacteria, during the antibiotic treatment (Figure 2G).

We evaluated species diversity in the mucosal and stool associated bacterial communities using the Inverse Simpson Index and found that there was no significant change in the diversity of the mucosal communities (Figure 3A). However there was a significant decrease in the diversity of the stool bacterial communities on Days 7 and 14, which returned to pre-antibiotic values by Day 28 (Figure 3B). The perturbation to the colonic bacterial communities was further demonstrated by principal coordinates analysis (PCoA), in which samples taken during the antibiotic treatment tended to cluster separately from those taken before or after the antibiotic treatment (Figure 3C/D), indicating disruption of the communities by the antibiotics. Together, these data demonstrate that the antibiotic treatments induced significant alterations to the diversity and composition of the bacterial communities in the colonic mucosa and lumen.

Antibiotic treatment reduces stool SCFA concentrations

SCFA are end products of bacterial fermentation that play major roles in regulating host health and immunity⁴⁰. Thus, we used GC-MS to measure the concentrations of acetate, propionate, butyrate, isobutyrate, valerate, and isovalerate in the stool of the RMs throughout the course of the study (Figure 4). Before the antibiotic treatment, we detected all six SCFA in the range of 0.98–8.3mM. Acetate was present in the highest concentrations (average 2.39 ± 1.11 mM), followed by butyrate (average 0.89 ± 0.7 mM), propionate (average 0.7 ± 0.86 mM), isovalerate (average 0.63 ± 0.37 mM), valerate (average 0.59 ± 0.47 mM), and isobutyrate (average 0.39 ± 0.21 mM). During the antibiotic treatment, the concentrations of all six SCFA significantly decreased as compared to baseline, but recovered to pre-antibiotic concentrations by Day 14. The observed reduction in SCFA concentrations in the stool was independent of the antibiotic used.

Antibiotic treatment is associated with altered colonic mucosal immunity

We used multicolor flow cytometry to evaluate immune profiles of colon biopsies throughout the course of the study. We found that there were significantly increased frequencies of neutrophils (as previously defined by our group in rhesus macaques as CD45+CD3-CD20-CD14+CD11b+ leukocytes⁴¹) during the antibiotic treatment that returned to normal levels after the antibiotic treatment had ended (Figure 5A/B) and that the neutrophils expressed lower levels of Caspase-3 during the antibiotic treatment (Figure 5C/D), indicating decreased levels of neutrophil apoptosis. This infiltration of neutrophils in the colonic mucosa was supported by RNA sequencing data demonstrating an increase in *CXCL8* expression (Figure 5E), the coding gene for IL-8, as well as an overall increase in the expression of genes within the IL-8 pathway from Day 3–14, and began to return to pre-antibiotic levels by Day 28, showing strong temporal alignment with the flow cytometry data (Figure 5F). However, not all of the treatment groups showed the same patterns of gene expression. Specifically, the enrofloxacin group showed a slight decrease in expression of *CXCL8* and the IL-8 pathway on Day 3, whereas the other groups showed an increase in expression on that day.

Specific bacteria and bacterial products in the GI tract can influence the polarization of CD4⁺ T cell subsets⁴⁰. Thus, we hypothesized that the antibiotic-induced microbiome perturbations could affect frequencies of key CD4⁺ T cell subsets. While the frequency of CD4⁺ T cells in the colonic mucosa remained stable throughout the course of the study (data not shown), we observed increased frequencies of CD4⁺ T cells producing IL-17 (Figure 6A/B) on Days 14, which reached significance by Day 28. Similarly, we observed increased frequencies of CD4⁺ T cells producing IL-22 (Figure 6C) on Days 14 and 28. Using RNA-seq, we demonstrated that there was increased expression of genes in the IL-17 pathway for all treatment groups on Day 14–28, which returned to pre-antibiotic levels afterward (Figure 6D).

To assess levels of systemic innate immune activation⁴², we measured plasma concentrations of sCD14. We observed a minor, but significant increase in plasma sCD14 during the antibiotic treatment, which then returned to baseline values by Day 14 (Figure 7). These data

demonstrate that, during and after the antibiotic treatment, there were significant changes in mucosal immunity indicative of immune activation.

Discussion

Antibiotics are a cornerstone of modern medicine, but unrestricted use has led to a variety of problems, including increased incidence of antibiotic resistant bacteria, as well as long-term alterations to the composition of colonic microbiota⁴³. Here, we demonstrated that oral administration of antibiotics disrupted colon mucosal and stool-associated bacterial communities in healthy rhesus macaques, and importantly, demonstrate for the first time specific alterations in mucosal immunity after antibiotics.

Of the antibiotic-induced microbiome alterations, the most prominent was increased abundances of *Enterobacteriaceae*. Expansion of enteric pathogens after antibiotic treatment has been observed previously in murine models, and is generally attributed to increased availability of carbohydrates after depletion of the native microbiota^{44, 45}. A further explanation may also be related to antibiotic resistance. Indeed, antibiotic resistant *Enterobacteriaceae* are a major emerging public health burden⁴⁶. We also observed increased abundances of *Akkermansia* during the antibiotic treatment. *A. muciniphila* is a well characterized intestinal mucolytic bacterium⁴⁷ and these bacteria have previously been shown to increase in abundance following antibiotic treatments¹⁸. Whether or not the increased abundance of *Akkermansia* was due to altered substrate pools is unclear, however it is important to note that increased abundances of mucolytic bacteria may alter mucous properties and thus may affect the integrity of the mucosal layers, and further studies understanding mechanisms of altered microbes after antibiotics are warranted.

While the effects on the microbiota varied between the different antibiotics, all four antibiotics elicited a dramatic reduction in stool SCFA concentrations. There are several explanations for this phenomenon. One explanation is that the antibiotics altered the bacterial metabolism, stalling SCFA production. Antibiotics are known to induce changes in bacterial metabolism and, while some of these responses are specific to the type of antibiotic used, others appear to be more generalized across multiple classes of antibiotics^{48, 49}. Such metabolic alterations induced by antibiotics, combined with continued utilization of SCFAs by the microbiota and host, may help explain the observed loss of SCFA production in this study. Recent evidence has demonstrated that propionate produced by commensal *Bacteroides* spp. inhibits the growth of pathogenic *Salmonella typhimurium* in murine models⁵⁰. Thus, the decreased stool SCFA concentrations in this study may have played a role in the expansion of *Enterobacteraceae* spp. However, further investigation is necessary to determine the precise cause and impacts of the decreased SCFA.

The immunological responses to the antibiotic-induced microbiome disruption also appear to be conserved across the different antibiotic classes. Indeed, we observed increased frequencies of neutrophils, Th17, and Th22 cells by flow cytometry either during or after the antibiotic treatment and these responses were conserved across all of the study groups. These alterations in mucosal immune status were further supported by RNA-seq demonstrating increased expression of genes in the IL-8 and IL-17 pathways. Neutrophils

are recruited to the sites of bacterial infections and are critical for protecting against pathogenic bacteria⁵¹. In the context of this study, it is possible that neutrophils were recruited to the colonic mucosa in response to the altered microbiota composition. We also demonstrated reduced neutrophil apoptosis during the antibiotic treatment. Increased neutrophil lifespan may contribute to mucosal inflammation through increased release of antimicrobial factors such as proteases and reactive oxygen species, which can disrupt the integrity of mucosal epithelial barriers⁵². This is supported by the increased plasma concentrations of sCD14 post-treatment, which has been extensively used as a biomarker of reduced mucosal epithelial integrity and translocation of microbes and microbial products from the intestinal lumen into the periphery³.

Neutrophils have also been shown to play a role in recruiting Th17 cells⁵³, and this is supported by the timing of the increase of Th17 cells and global gene expression patterns in our study. Th17 cells are important for maintaining mucosal homeostasis and for protection against intestinal pathogens⁵⁴. Thus, the observed increase in Th17 cells in this study was likely also in response to the antibiotic-induced microbiota alterations. However, it is also important to note that approximately the same time that we observed increased Th17 cells (D14-D28), we also observed increased frequencies of Th22 cells, as well as CD4+ T cells producing both IL-17 and IL-22. Th22 cells (and IL-22) are important for protecting against pathogenic bacteria⁵⁵, but also promote epithelial regeneration and repair⁵⁶. Thus, the observed increase of Th17 and Th22 cells could also be in response to mucosal dysfunction and thus important for restoration of the colonic epithelium during the resolution of inflammation caused by the influx of neutrophils. The precise mechanisms underlying these changes in mucosal immunity during antibiotic treatment require further study.

A caveat of these studies is the very small group size in each antibiotic category. This study was initially designed as a pilot study to determine which antibiotics should be focused on for nonhuman primate research. Given the difference in mechanisms of activity of each antibiotic, it was somewhat surprising how conserved the microbial and immune responses to all the groups was. Thus, we chose to group all antibiotics for analysis to focus on these conserved mechanisms. However, future studies focused on individual antibiotics and potential disparate effects are seen in larger treatment groups will be important for future studies.

In summary, these data demonstrate that antibiotic treatments disrupt colonic bacterial communities and promote mucosal inflammation and epithelial disruption in healthy rhesus macaques. Macaques are the most biologically relevant animal model for studies of human immunology and are used as a model for a variety of diseases, in particular HIV infection^{9, 57}. HIV and pathogenic SIV infection are associated with dysbiosis of the intestinal microbiota and significant dysfunction of the mucosa independent of antibiotics^{12, 58, 59}. Thus, antibiotic use in HIV-infected individuals might exacerbate these conditions and contribute to further immune activation. Further, antibiotic use in studies of SIV infection that involve evaluations of mucosal immunity and the intestinal microbiota can have dramatic impacts on the results. These data suggest that antibiotic use should be avoided unless absolutely necessary in such studies.

Acknowledgements

We thank all veterinary staff of the Washington National Primate Research Center for conducting the animal studies. These studies in part were funded with support from the WaNPRC NIH core grant P51 OD010425-51, and partially by NIH grants 1R01AI128782 and 1R01DK112254 to N.R.K. and amfAR 109222-58-RGRL to C.M.C.-J.A.M. was supported by K01OD024876. We also thank the Case Western Applied Functional Genomics Core.

References

1. Thaiss CA, Levy M, Suez J, Elinav E. The interplay between the innate immune system and the microbiota. *Curr Opin Immunol* 2014; 26: 41–48. [PubMed: 24556399]
2. Hullar MA, Fu BC. Diet, the gut microbiome, and epigenetics. *Cancer J* 2014; 20(3): 170–175. [PubMed: 24855003]
3. Brenchley JM, Price DA, Schacker TW, Asher TE, Silvestri G, Rao S et al. Microbial translocation is a cause of systemic immune activation in chronic HIV infection. *Nat Med* 2006; 12(12): 1365–1371. [PubMed: 17115046]
4. Dillon SM, Lee EJ, Kotter CV, Austin GL, Gianella S, Siewe B et al. Gut dendritic cell activation links an altered colonic microbiome to mucosal and systemic T-cell activation in untreated HIV-1 infection. *Mucosal Immunol* 2016; 9(1): 24–37. [PubMed: 25921339]
5. Jiang W, Lederman MM, Hunt P, Sieg SF, Haley K, Rodriguez B et al. Plasma levels of bacterial DNA correlate with immune activation and the magnitude of immune restoration in persons with antiretroviral-treated HIV infection. *J Infect Dis* 2009; 199(8): 1177–1185. [PubMed: 19265479]
6. Sandler NG, Wand H, Roque A, Law M, Nason MC, Nixon DE et al. Plasma levels of soluble CD14 independently predict mortality in HIV infection. *J Infect Dis* 2011; 203(6): 780–790. [PubMed: 21252259]
7. Vujkovic-Cvijin I, Dunham RM, Iwai S, Maher MC, Albright RG, Broadhurst MJ et al. Dysbiosis of the gut microbiota is associated with HIV disease progression and tryptophan catabolism. *Sci Transl Med* 2013; 5(193): 193ra191.
8. Gardner MB, Luciw PA. Macaque models of human infectious disease. *Ilar j* 2008; 49(2): 220–255. [PubMed: 18323583]
9. Messaoudi I, Estep R, Robinson B, Wong SW. Nonhuman primate models of human immunology. *Antioxid Redox Signal* 2011; 14(2): 261–273. [PubMed: 20524846]
10. Veazey RS, Lackner AA. Nonhuman Primate Models and Understanding the Pathogenesis of HIV Infection and AIDS. *Ilar j* 2017; 58(2): 160–171. [PubMed: 29228218]
11. Ericson AJ, Lauck M, Mohns MS, DiNapoli SR, Mutschler JP, Greene JM et al. Microbial Translocation and Inflammation Occur in Hyperacute Immunodeficiency Virus Infection and Compromise Host Control of Virus Replication. *PLoS Pathog* 2016; 12(12): e1006048. [PubMed: 27926931]
12. Handley SA, Desai C, Zhao G, Droit L, Monaco CL, Schroeder AC et al. SIV Infection-Mediated Changes in Gastrointestinal Bacterial Microbiome and Virome Are Associated with Immunodeficiency and Prevented by Vaccination. *Cell Host Microbe* 2016; 19(3): 323–335. [PubMed: 26962943]
13. Handley SA, Thackray LB, Zhao G, Presti R, Miller AD, Droit L et al. Pathogenic simian immunodeficiency virus infection is associated with expansion of the enteric virome. *Cell* 2012; 151(2): 253–266. [PubMed: 23063120]
14. Klase Z, Ortiz A, Deleage C, Mudd JC, Quinones M, Schwartzman E et al. Dysbiotic bacteria translocate in progressive SIV infection. *Mucosal Immunol* 2015; 8(5): 1009–1020. [PubMed: 25586559]
15. Moeller AH, Shilts M, Li Y, Rudicell RS, Lonsdorf EV, Pusey AE et al. SIV-induced instability of the chimpanzee gut microbiome. *Cell Host Microbe* 2013; 14(3): 340–345. [PubMed: 24034619]
16. Evans TI, Li H, Schafer JL, Klatt NR, Hao XP, Traslavina RP et al. SIV-induced Translocation of Bacterial Products in the Liver Mobilizes Myeloid Dendritic and Natural Killer Cells Associated With Liver Damage. *J Infect Dis* 2016; 213(3): 361–369. [PubMed: 26238685]

17. Hensley-McBain T, Zevin AS, Manuzak J, Smith E, Gile J, Miller C et al. Effects of Fecal Microbial Transplantation on Microbiome and Immunity in Simian Immunodeficiency Virus-Infected Macaques. *J Virol* 2016; 90(10): 4981–4989. [PubMed: 26937040]
18. Dubourg G, Lagier JC, Armougom F, Robert C, Audoly G, Papazian L et al. High-level colonisation of the human gut by Verrucomicrobia following broad-spectrum antibiotic treatment. *Int J Antimicrob Agents* 2013; 41(2): 149–155. [PubMed: 23294932]
19. Knoop KA, Gustafsson JK, McDonald KG, Kulkarni DH, Kassel R, Newberry RD. Antibiotics promote the sampling of luminal antigens and bacteria via colonic goblet cell associated antigen passages. *Gut Microbes* 2017; 8(4): 400–411. [PubMed: 28267403]
20. Knoop KA, McDonald KG, Kulkarni DH, Newberry RD. Antibiotics promote inflammation through the translocation of native commensal colonic bacteria. *Gut* 2016; 65(7): 1100–1109. [PubMed: 26045138]
21. Candon S, Perez-Arroyo A, Marquet C, Valette F, Foray AP, Pelletier B et al. Antibiotics in early life alter the gut microbiome and increase disease incidence in a spontaneous mouse model of autoimmune insulin-dependent diabetes. *PLoS One* 2015; 10(5): e0125448. [PubMed: 25970503]
22. Zevin AS, Hensley-McBain T, Miller C, Smith E, Langevin S, Klatt NR. Antibiotic treatment disrupts bacterial communities in the colon and rectum of simian immunodeficiency virus-infected macaques. *FEMS Microbiol Lett* 2017; 364(23).
23. Kalman D, Barriere SL. Review of the pharmacology, pharmacokinetics, and clinical use of cephalosporins. *Tex Heart Inst J* 1990; 17(3): 203–215. [PubMed: 15227172]
24. Dhawan VK, Thadepalli H. Clindamycin: a review of fifteen years of experience. *Rev Infect Dis* 1982; 4(6): 1133–1153. [PubMed: 6818656]
25. Lell B, Kremsner PG. Clindamycin as an antimalarial drug: review of clinical trials. *Antimicrob Agents Chemother* 2002; 46(8): 2315–2320. [PubMed: 12121898]
26. Caccio S, Pinter E, Fantini R, Mezzaroma I, Pozio E. Human infection with *Cryptosporidium felis*: case report and literature review. *Emerg Infect Dis* 2002; 8(1): 85–86. [PubMed: 11749756]
27. Kim J, Coble DJ, Salyards GW, Bower JK, Rinaldi WJ, Plauche GB et al. Antimicrobial Use for and Resistance of Zoonotic Bacteria Recovered from Nonhuman Primates. *Comp Med* 2017; 67(1): 79–86. [PubMed: 28222842]
28. Walters W, Hyde ER, Berg-Lyons D, Ackermann G, Humphrey G, Parada A et al. Improved Bacterial 16S rRNA Gene (V4 and V4–5) and Fungal Internal Transcribed Spacer Marker Gene Primers for Microbial Community Surveys. *mSystems* 2016; 1(1).
29. Caporaso JG, Kuczynski J, Stombaugh J, Bittinger K, Bushman FD, Costello EK et al. QIIME allows analysis of high-throughput community sequencing data. *Nat Methods* 2010; 7(5): 335–336. [PubMed: 20383131]
30. Mahe F, Rognes T, Quince C, de Vargas C, Dunthorn M. Swarm: robust and fast clustering method for amplicon-based studies. *PeerJ* 2014; 2: e593. [PubMed: 25276506]
31. Pruesse E, Quast C, Knittel K, Fuchs BM, Ludwig W, Peplies J et al. SILVA: a comprehensive online resource for quality checked and aligned ribosomal RNA sequence data compatible with ARB. *Nucleic Acids Res* 2007; 35(21): 7188–7196. [PubMed: 17947321]
32. Kim D, Langmead B, Salzberg SL. HISAT: a fast spliced aligner with low memory requirements. *Nat Methods* 2015; 12(4): 357–360. [PubMed: 25751142]
33. Li H, Handsaker B, Wysoker A, Fennell T, Ruan J, Homer N et al. The Sequence Alignment/Map format and SAMtools. *Bioinformatics* 2009; 25(16): 2078–2079. [PubMed: 19505943]
34. Liao Y, Smyth GK, Shi W. featureCounts: an efficient general purpose program for assigning sequence reads to genomic features. *Bioinformatics* 2014; 30(7): 923–930. [PubMed: 24227677]
35. Robinson MD, McCarthy DJ, Smyth GK. edgeR: a Bioconductor package for differential expression analysis of digital gene expression data. *Bioinformatics* 2010; 26(1): 139–140. [PubMed: 19910308]
36. Hanzelmann S, Castelo R, Guinney J. GSEA: gene set variation analysis for microarray and RNA-seq data. *BMC Bioinformatics* 2013; 14: 7. [PubMed: 23323831]
37. Ritchie ME, Phipson B, Wu D, Hu Y, Law CW, Shi W et al. limma powers differential expression analyses for RNA-sequencing and microarray studies. *Nucleic Acids Res* 2015; 43(7): e47. [PubMed: 25605792]

38. Wickham H Ggplot2 : elegant graphics for data analysis. Springer: New York, 2009, viii, 212 p.pp.
39. Yasuda K, Oh K, Ren B, Tickle TL, Franzosa EA, Wachtman LM et al. Biogeography of the intestinal mucosal and luminal microbiome in the rhesus macaque. *Cell Host Microbe* 2015; 17(3): 385–391. [PubMed: 25732063]
40. Park J, Kim M, Kang SG, Jannasch AH, Cooper B, Patterson J et al. Short-chain fatty acids induce both effector and regulatory T cells by suppression of histone deacetylases and regulation of the mTOR-S6K pathway. *Mucosal Immunol* 2015; 8(1): 80–93. [PubMed: 24917457]
41. Hensley-McBain T, Berard AR, Manuzak JA, Miller CJ, Zevin AS, Polacino P et al. Intestinal damage precedes mucosal immune dysfunction in SIV infection. *Mucosal Immunol* 2018; 11(5): 1429–1440. [PubMed: 29907866]
42. Shive CL, Jiang W, Anthony DD, Lederman MM. Soluble CD14 is a nonspecific marker of monocyte activation. *Aids* 2015; 29(10): 1263–1265. [PubMed: 26035325]
43. Korpela K, Salonen A, Virta LJ, Kekkonen RA, Forslund K, Bork P et al. Intestinal microbiome is related to lifetime antibiotic use in Finnish pre-school children. *Nat Commun* 2016; 7: 10410. [PubMed: 26811868]
44. Faber F, Tran L, Byndloss MX, Lopez CA, Velazquez EM, Kerrinnes T et al. Host-mediated sugar oxidation promotes post-antibiotic pathogen expansion. *Nature* 2016; 534(7609): 697–699. [PubMed: 27309805]
45. Ng KM, Ferreyra JA, Higginbottom SK, Lynch JB, Kashyap PC, Gopinath S et al. Microbiota-liberated host sugars facilitate post-antibiotic expansion of enteric pathogens. *Nature* 2013; 502(7469): 96–99. [PubMed: 23995682]
46. Savard P, Perl TM. A call for action: managing the emergence of multidrug-resistant Enterobacteriaceae in the acute care settings. *Curr Opin Infect Dis* 2012; 25(4): 371–377. [PubMed: 22766646]
47. van Passel MW, Kant R, Zoetendal EG, Plugge CM, Derrien M, Malfatti SA et al. The genome of *Akkermansia muciniphila*, a dedicated intestinal mucin degrader, and its use in exploring intestinal metagenomes. *PLoS One* 2011; 6(3): e16876. [PubMed: 21390229]
48. Belenky P, Ye JD, Porter CB, Cohen NR, Lobritz MA, Ferrante T et al. Bactericidal Antibiotics Induce Toxic Metabolic Perturbations that Lead to Cellular Damage. *Cell Rep* 2015; 13(5): 968–980. [PubMed: 26565910]
49. Zampieri M, Zimmermann M, Claassen M, Sauer U. Nontargeted Metabolomics Reveals the Multilevel Response to Antibiotic Perturbations. *Cell Rep* 2017; 19(6): 1214–1228. [PubMed: 28494870]
50. Jacobson A, Lam L, Rajendram M, Tamburini F, Honeycutt J, Pham T et al. A Gut Commensal-Produced Metabolite Mediates Colonization Resistance to Salmonella Infection. *Cell Host Microbe* 2018; 24(2): 296–307.e297. [PubMed: 30057174]
51. Wera O, Lancellotti P, Oury C. The Dual Role of Neutrophils in Inflammatory Bowel Diseases. *J Clin Med* 2016; 5(12).
52. Elbim C, Monceaux V, Mueller YM, Lewis MG, Francois S, Diop O et al. Early divergence in neutrophil apoptosis between pathogenic and nonpathogenic simian immunodeficiency virus infections of nonhuman primates. *J Immunol* 2008; 181(12): 8613–8623. [PubMed: 19050281]
53. Pelletier M, Maggi L, Micheletti A, Lazzeri E, Tamassia N, Costantini C et al. Evidence for a cross-talk between human neutrophils and Th17 cells. *Blood* 2010; 115(2): 335–343. [PubMed: 19890092]
54. Wang Z, Friedrich C, Hagemann SC, Korte WH, Goharani N, Cording S et al. Regulatory T cells promote a protective Th17-associated immune response to intestinal bacterial infection with *C. rodentium*. *Mucosal Immunol* 2014; 7(6): 1290–1301. [PubMed: 24646939]
55. Basu R, O’Quinn DB, Silberger DJ, Schoeb TR, Fouser L, Ouyang W et al. Th22 cells are an important source of IL-22 for host protection against enteropathogenic bacteria. *Immunity* 2012; 37(6): 1061–1075. [PubMed: 23200827]
56. Kim CJ, Nazli A, Rojas OL, Chege D, Alidina Z, Huibner S et al. A role for mucosal IL-22 production and Th22 cells in HIV-associated mucosal immunopathogenesis. *Mucosal Immunol* 2012; 5(6): 670–680. [PubMed: 22854709]

57. Hatzioannou T, Evans DT. Animal models for HIV/AIDS research. *Nat Rev Microbiol* 2012; 10(12): 852–867. [PubMed: 23154262]
58. Brenchley JM. Mucosal immunity in human and simian immunodeficiency lentivirus infections. *Mucosal Immunol* 2013; 6(4): 657–665. [PubMed: 23549448]
59. Dillon SM, Lee EJ, Kotter CV, Austin GL, Dong Z, Hecht DK et al. An altered intestinal mucosal microbiome in HIV-1 infection is associated with mucosal and systemic immune activation and endotoxemia. *Mucosal Immunol* 2014; 7(4): 983–994. [PubMed: 24399150]

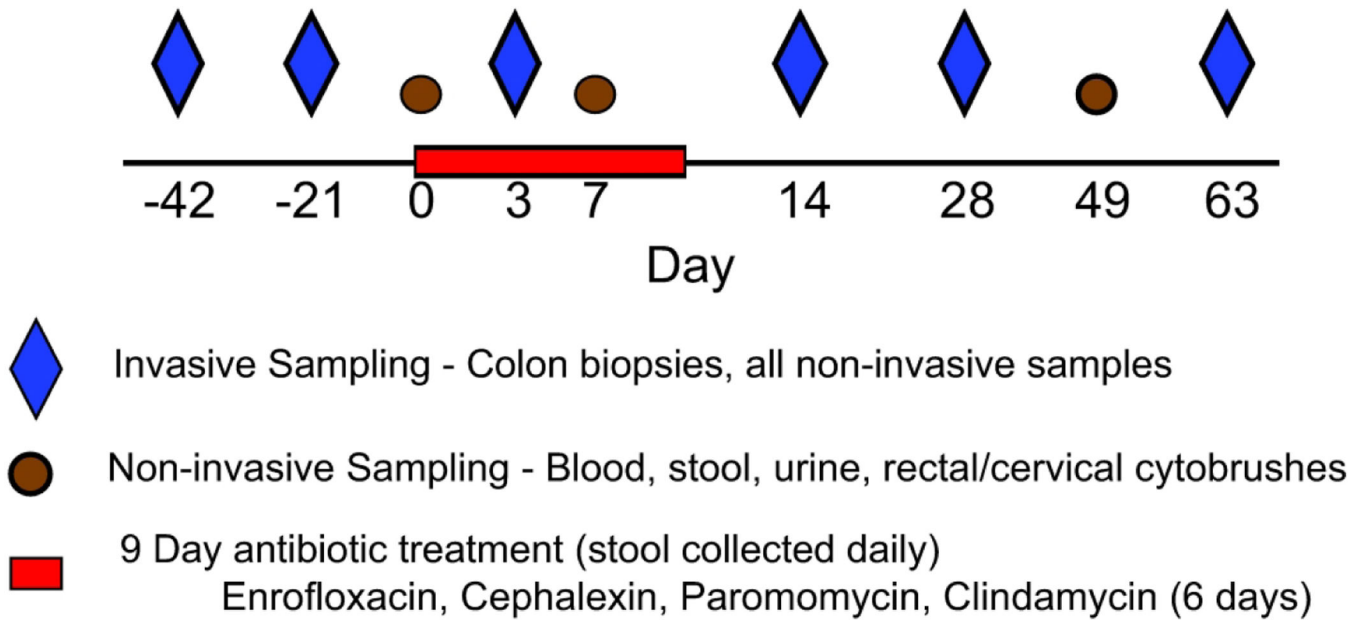


Figure 1. Study Schedule.

Animals (n=3 per group) were treated with enrofloxacin, cephalexin or paromomycin for nine days, or clindamycin for six days. Two sets of samples were collected prior to the treatment. During the treatments, non-invasive samples were collected three times and mucosal samples collected once. Animals were tracked for 63 days after initiation of the antibiotic treatments.

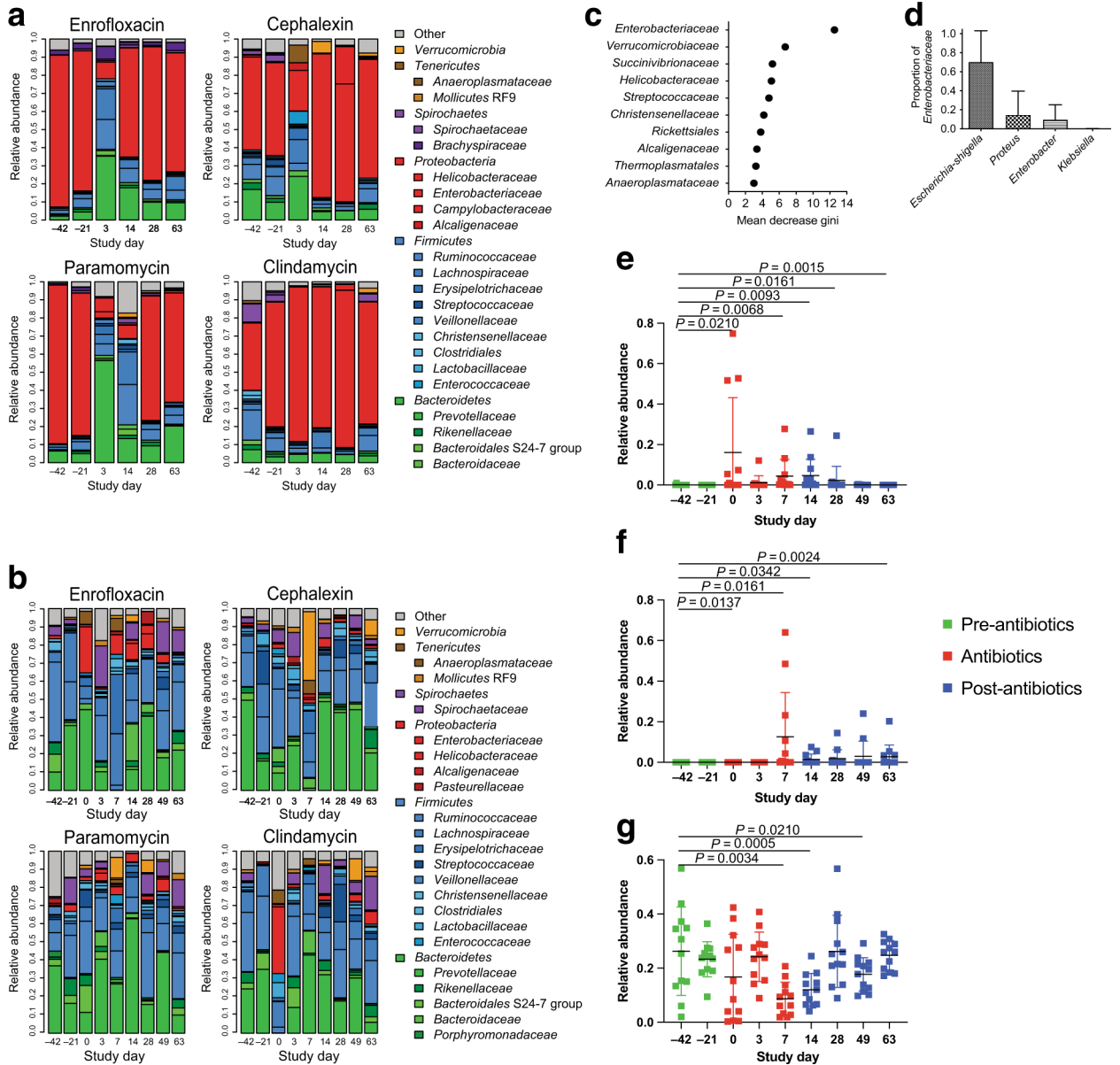


Figure 2. Bacterial community composition of the colonic mucosa throughout the antibiotic treatments.

(A) Mucosal bacterial communities of all animals showed a high abundance of *Helicobacteraceae* prior to the antibiotic treatment. The antibiotics disrupted the mucosal bacterial communities, but clindamycin showed no impact on the predominant *Helicobacteraceae*. (B) Stool-associated bacterial communities of all of the animals were highly diverse, predominated by bacteria from the phyla Firmicutes and Bacteroides. Each antibiotic disrupted these communities, but the effects on community composition varied between the different antibiotics. (C) Random Forest analysis demonstrated that *Enterobacteriaceae* were the most strongly discriminating bacterial group in the stool bacterial communities at time points when antibiotics were being administered. (D) Other discriminating groups included *Verrucomicrobiaceae*, *Helicobacteraceae*, and

Streptococcaeae, among others. The most abundant genera of *Enterobacteriaceae* included *Escherichia*, *Proteus*, and *Enterobacter* with a small proportion of *Klebsiella*. **(E)** The relative abundance of *Enterobacteriaceae* in the stool bacterial communities increased rapidly upon initiation of the antibiotic treatments (Day 0–7), persisted in some animals until Day 14, and then returned to pre-antibiotic levels by Day 49. **(F)** *Akkermansia*, detected in the stool bacterial communities, increased in relative abundance near the end of the antibiotic treatment and then persisted through the end of the study. **(G)** *Ruminococcaceae* displayed decreased relative abundance on Days 7 and 14, and increased back to pre-antibiotic levels on Day 28. **(E-G)** Green points indicate samples taken prior to the antibiotic treatment, red points indicate samples during the antibiotic treatment, and blue points indicate samples taken after cessation of the antibiotic treatment. Statistics were performed across all antibiotic treatment groups using a Wilcoxon signed-rank test and corrected for multiple comparisons using a post-hoc Bonferroni correction.

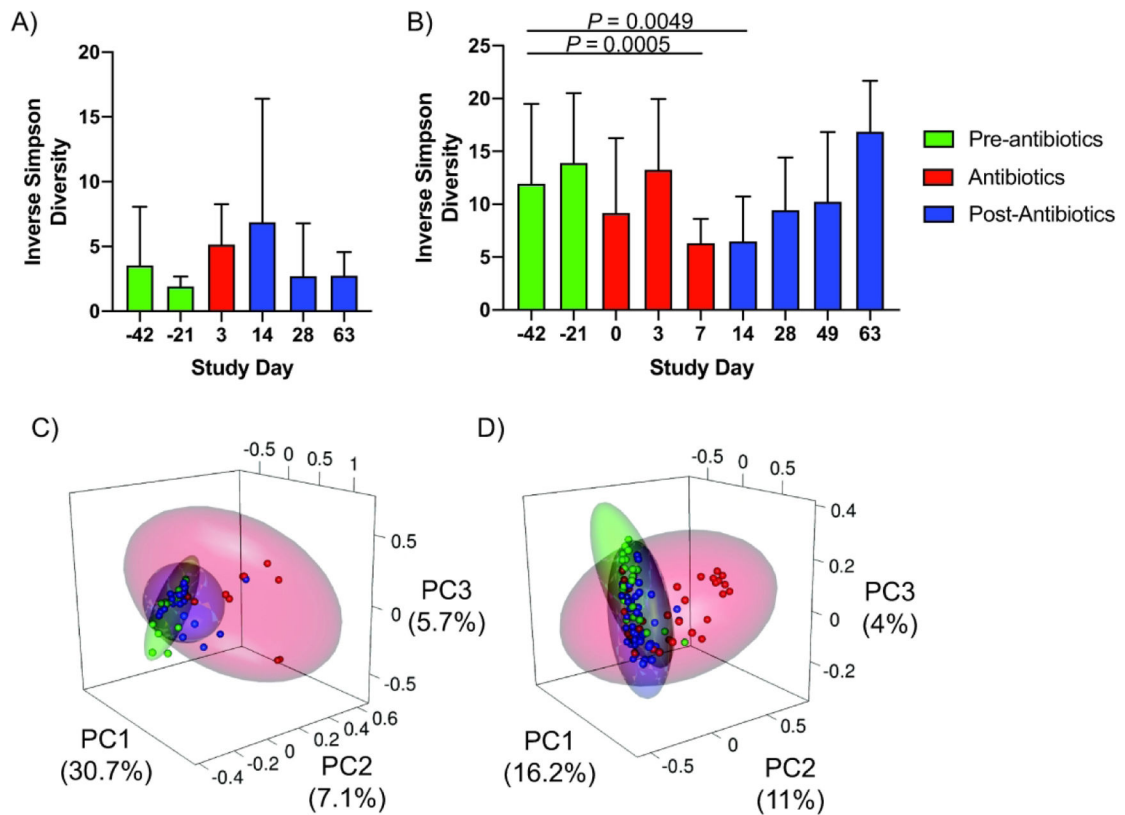


Figure 3. Antibiotics alter diversity of mucosal and stool bacterial communities.

(A) Species diversity, as measured by the Inverse Simpson Index, was altered by antibiotic treatment across all animals in the four antibiotic treatment groups. The colonic mucosa showed increased species diversity during (Day 3) and shortly after (Day 14) the antibiotic treatments. (B) Stool communities showed reduced diversity during (Days 0, 3, 7) and shortly after (Day 14) the antibiotic treatment. (C-D) Principal coordinates analysis confirmed that the antibiotics disrupted the community composition in the mucosa (C) and stool (D) during the antibiotic treatment. Green points indicate samples taken prior to the antibiotic treatment, red points indicate samples during the antibiotic treatment, and blue points indicate samples taken after cessation of the antibiotic treatment. Statistics were performed across all groups using a Wilcoxon signed-rank test and corrected for multiple comparisons using a post-hoc Bonferroni correction.

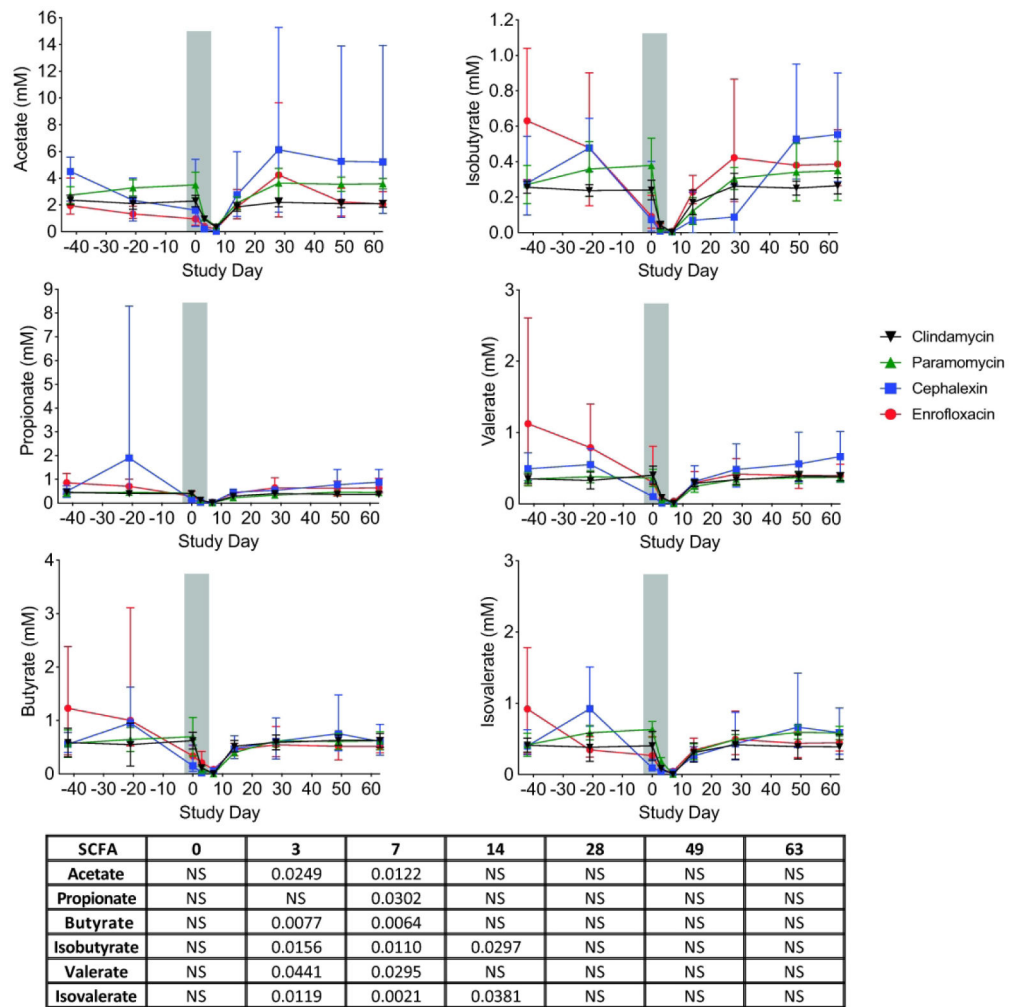


Figure 4. Concentrations of SCFA decrease during antibiotic treatment.

Across all four antibiotic treatment groups, stool concentrations of the SCFA acetate, propionate, butyrate, isobutyrate, valerate, and isoavaerate were significantly reduced during the antibiotic treatment (indicated by gray bar) and rapidly returned to pre-antibiotic levels following cessation of the antibiotic treatments. Enrofloxacin – red circles, cephalixin – blue squares, paramomycin – green triangles, clindamycin – black upside-down triangles. The table below shows *P* values that were determined using a paired-t test with Bonferroni Correction for for multiple comparisons (NS: not significant). Statistics were performed across all antibiotic treatment groups.

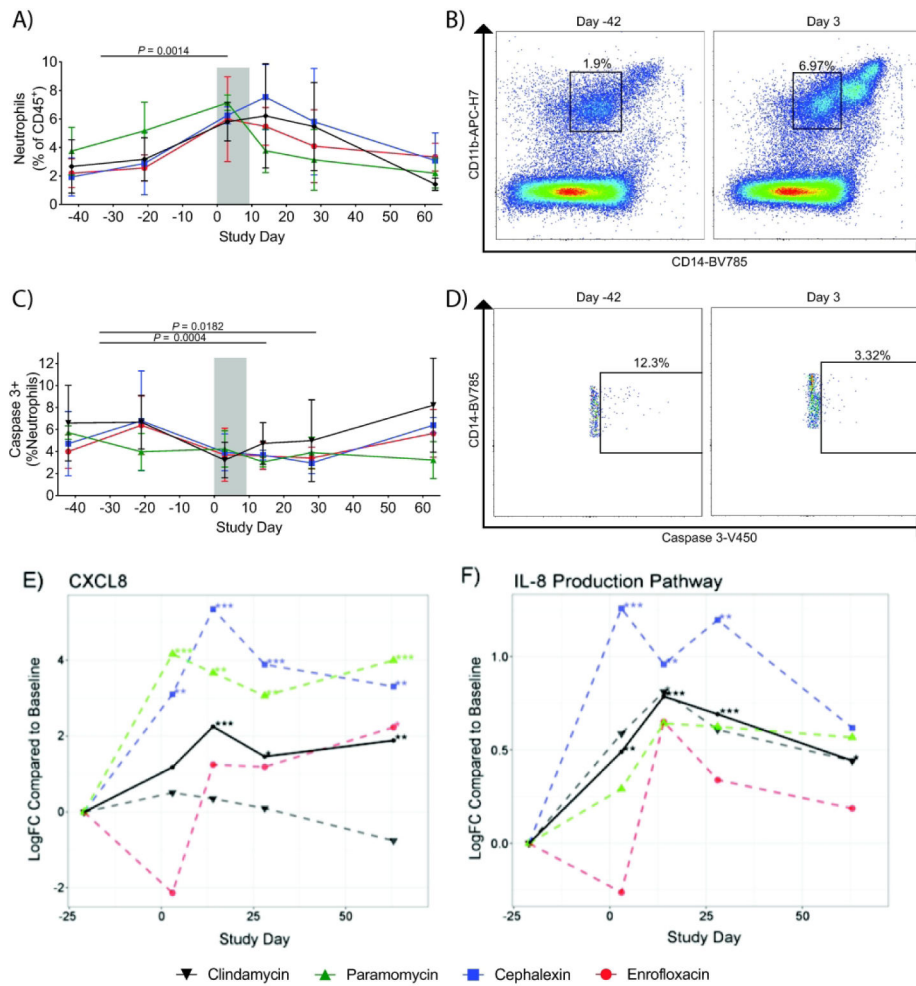


Figure 5. Neutrophils infiltrate the colonic mucosa during antibiotic treatment.

(A) In all treatment groups, flow cytometry analysis demonstrated a significant increase of neutrophils in the colonic mucosa during the antibiotic treatment (indicated by the gray bar), which persisted to Day 14 and then returned to pre-antibiotic levels by Day 28–63. (B) Representative flow cytometry plots demonstrating accumulation of neutrophils on Day 3 of the antibiotic treatment. Neutrophils were specifically identified as CD45⁺CD3⁺CD20⁻CD14⁺CD11b⁺ leukocytes. CD11b⁺CD14⁺ cells were specifically gated out in order to exclude monocytes from the analysis. (C/D) We observed a significant decrease in Caspase-3⁺ neutrophils at days 14 and 28, which returned to pre-antibiotic levels by Day 63. (E-F) RNA-seq analysis demonstrated increased expression of *cxcl8*, the gene encoding IL-8 (E), as well as the IL-8 production pathway (F) with strong temporal alignment with the neutrophil infiltration observed through the flow cytometry analysis. Interestingly, the enrofloxacin group showed reduced expression of *cxcl8* and the IL-8 production pathway on Day 3, but increased expression on Day 14. Enrofloxacin – red circles, cephalixin – blue squares, paramomycin – green triangles, clindamycin – black upside-down triangles. *P* values were determined using a paired-t test with Bonferroni Correction for multiple comparisons. Statistics were performed across all antibiotic treatment groups.

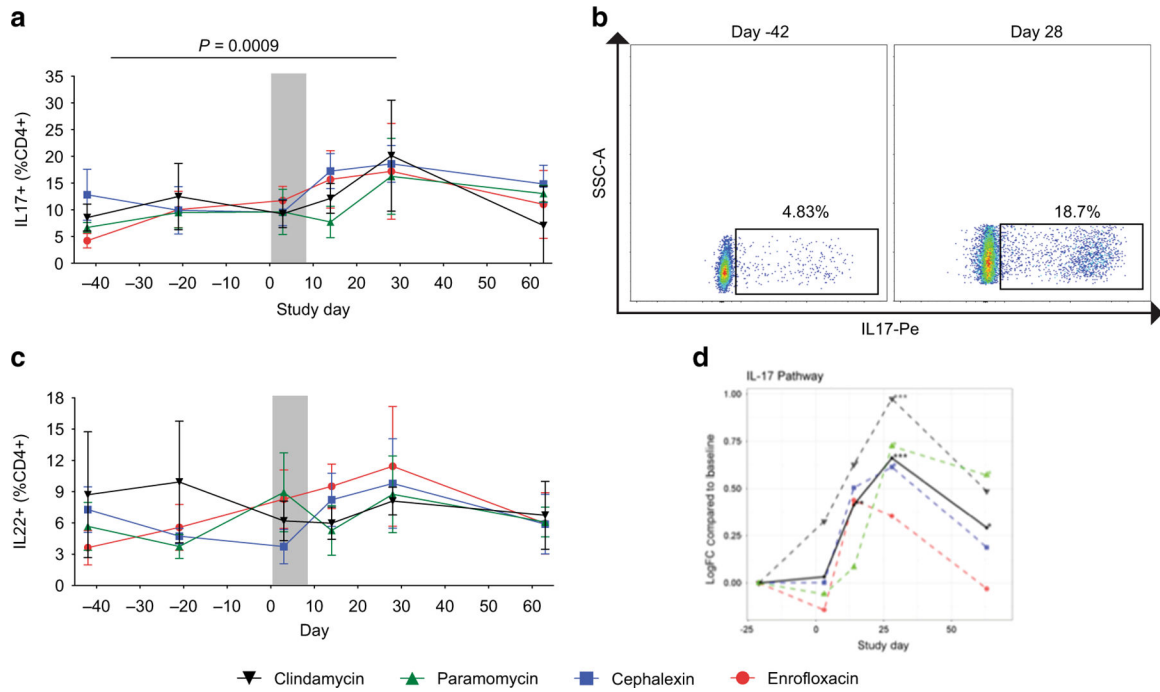


Figure 6. IL-17 producing CD4+ T cells increase in the colonic mucosa following the antibiotic treatment.

(A) Flow cytometry analysis demonstrated an increase of IL-17 producing CD4+ T cells (defined as CD45+CD3+CD4+IL17+) in the colonic mucosa after the antibiotic treatment (indicated by the gray bar) at Day 14 and a significant increase at Day 28, which returned to pre-antibiotic values by Day 63. (B) Representative flow cytometry plots demonstrating increased frequency of IL-17-producing CD4+ T cells on Day 28. (C) We observed an increase in the frequency of IL-22-producing CD4+ T cells. (D) mRNA-seq analysis similarly demonstrated increased expression of genes in the IL-17 pathway on Day 14–28 after the antibiotic treatment. Enrofloxacin – red circles, cephalalexin – blue squares, paramomycin – green triangles, clindamycin – black upside-down triangles. *P* values were determined using a paired-t test with Bonferroni Correction for multiple comparisons. Statistics were performed across all antibiotic treatment groups.

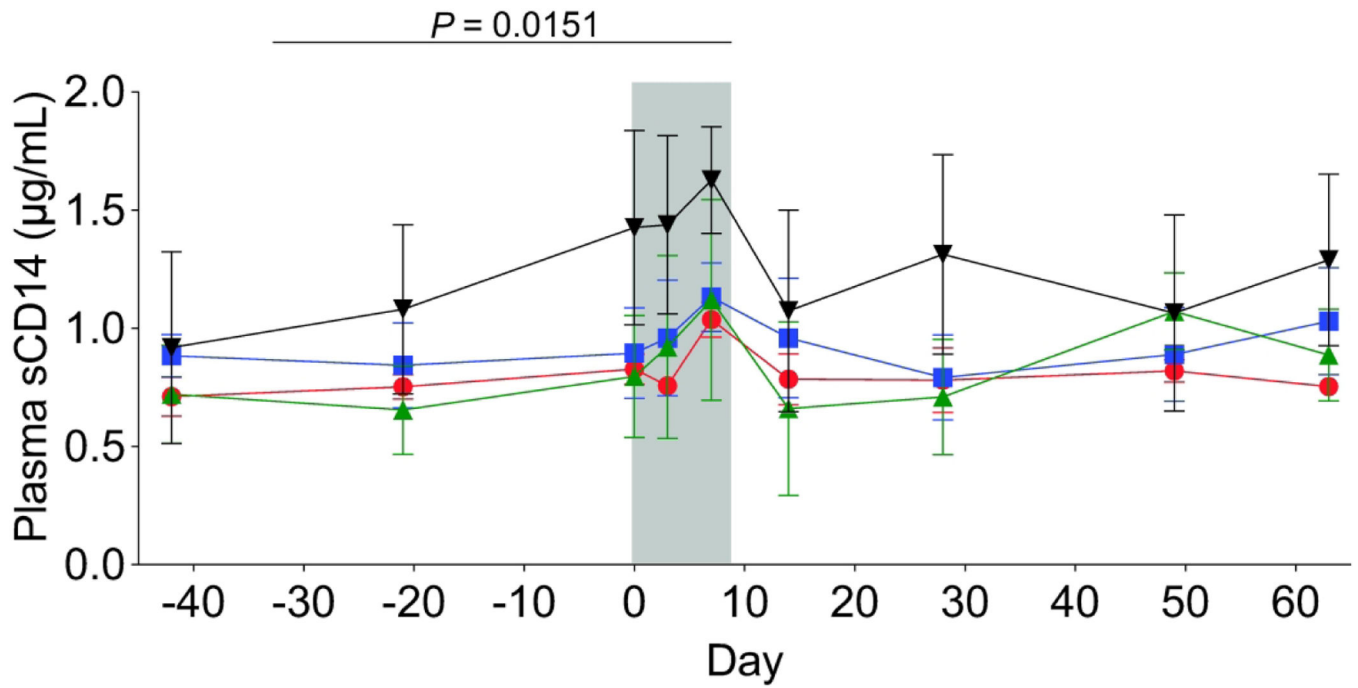


Figure 7. Plasma concentrations of sCD14 increased during antibiotic treatment.

Across all treatment groups, we observed an increase in plasma concentrations of sCD14 during the antibiotic treatment (indicated by the gray bar), which reached significance at Day 7. Plasma sCD14 levels returned to pre-antibiotic values following cessation of antibiotics. These data support an inflammatory response during the antibiotic treatment. Enrofloxacin – red circles, cephalixin – blue squares, paromomycin – green triangles, clindamycin – black upside-down triangles. *P* values were determined using a paired-t test with Bonferroni Correction for multiple comparisons. Statistics were performed across all antibiotic treatment groups.